PCP
PLANT & CELL PHYSIOLOGY

BBX24 Interacts with JAZ3 to Promote Growth by Reducing DELLA Activity in Shade Avoidance

Maite Saura-Sánchez[1], Tai Sabrina Chiriotto[1], Jimena Cascales[1], Gabriel Gómez-Ocampo[1], Jorge Hernández-García[2], Zheng Li[3], José Luis Pruneda-Paz[3], Miguel Angel Blázquez[2] and Javier Francisco Botto[1,*]

[1]Instituto de Investigaciones Fisiológicas y Ecológicas Vinculadas a la Agricultura (IFEVA), Consejo Nacional de Investigaciones Científicas y Técnicas (CONICET), Facultad de Agronomía, Universidad de Buenos Aires (UBA), Av. San Martín 4453, Ciudad Autónoma de Buenos Aires C1417DSE, Argentina
[2]Instituto de Biología Molecular y Celular de Plantas, Consejo Superior de Investigaciones Científicas–Universidad Politécnica de Valencia, C/Ingeniero Fausto Elio s/n, Valencia 46022, Spain
[3]Section of Cell and Developmental Biology, Division of Biological Sciences, University of California San Diego, 9500 Gilman Drive, La Jolla, CA 92093-0348, USA

*Corresponding author: E-mail, botto@agro.uba.ar

(Received 24 August 2022; Accepted 26 January 2023)

Regular Paper

Shade avoidance syndrome (SAS) is a strategy of major adaptive significance and typically includes elongation of the stem and petiole, leaf hyponasty, reduced branching and phototropic orientation of the plant shoot toward canopy gaps. Both cryptochrome 1 and phytochrome B (phyB) are the major photoreceptors that sense the reduction in the blue light fluence rate and the low red:far-red ratio, respectively, and both light signals are associated with plant density and the resource reallocation when SAS responses are triggered. The B-box (BBX)-containing zinc finger transcription factor BBX24 has been implicated in the SAS as a regulator of DELLA activity, but this interaction does not explain all the observed BBX24-dependent regulation in shade light. Here, through a combination of transcriptional meta-analysis and large-scale identification of BBX24-interacting transcription factors, we found that JAZ3, a jasmonic acid signaling component, is a direct target of BBX24. Furthermore, we demonstrated that joint loss of BBX24 and JAZ3 function causes insensitivity to DELLA accumulation, and the defective shade-induced elongation in this mutant is rescued by loss of DELLA or phyB function. Therefore, we propose that JAZ3 is part of the regulatory network that controls the plant growth in response to shade, through a mechanism in which BBX24 and JAZ3 jointly regulate DELLA activity. Our results provide new insights into the participation of BBX24 and JA signaling in the hypocotyl shade avoidance response in *Arabidopsis*.

Keywords: BBX24 • DELLAs • JAZ3 • Phytochrome B (phyB) • Shade avoidance syndrome (SAS)

Introduction

Shade avoidance syndrome (SAS) is a strategy of major adaptive significance to respond to the presence of neighbors, well before shading occurs, by the elongation of stems and petioles and leaf hyponasty among other responses (Casal 2013, Ballaré and Pierik 2017). When true shading occurs, the transmitted light is especially depleted at red and blue wavelengths, due to absorption by chlorophylls, reducing the photosynthetically active radiation (PAR). The reduction in the red:far-red (R:FR) ratio and the reduction in the blue light fluence rate inactivate phytochrome B (phyB) and cryptochrome 1, respectively, which induce the SAS responses in shade. At the molecular level, the transcription factors, PHYTOCHROME INTERACTING FACTORS (PIFs), promote the shade-induced gene expression, and the CONSTITUTIVE PHOTOMORPHOGENIC 1/SUPPRESSOR OF phyA-105 (COP1/SPA) ubiquitin E3 ligase complex controls the stability of proteins to optimize the growth reconfiguration and the reallocation of resources in shade. Furthermore, hormonal regulatory networks including auxin, gibberellins (GA) and brassinosteroids contribute to triggering SAS signaling and adjusting plant growth in shade (Yang and Li 2017).

The GA promotes plant growth triggering the degradation of DELLA proteins, which function as master growth repressors of GA signaling (Phokas and Coates 2021). The binding of bioactive GA to the GA-INSENSITIVE DWARF1 (GID1) receptor promotes the interaction of the complex GA-GID1 with DELLAs (Ueguchi-Tanaka et al. 2005, Nakajima et al. 2006). DELLAs are subsequently poly-ubiquitinated by the E3 ubiquitin ligases [e.g. SLEEPY1 and COP1] and thus targeted for destruction in the 26S proteasome (McGinnis et al. 2003, Blanco-Touriñán et al. 2020). Low R:FR ratios and low blue signals typically of real canopies reduce the stability of DELLAs, likely as a consequence of increased gibberellin levels (Djakovic-Petrovic et al. 2007). Mutants with stable DELLA versions show reduced responses to shade, and mutants combining loss-of-function alleles at multiple DELLA have elongated stems even in the absence of shade (Djakovic-Petrovic et al. 2007). At the molecular level, the

Plant Cell Physiol. 64(5): 474–485 (2023) doi:https://doi.org/10.1093/pcp/pcad011, Advance Access publication on 27 January 2023, available online at https://academic.oup.com/pcp

physical interaction between the first conserved heptad leucine repeat of DELLA and the PIF DNA recognition domain prevents PIFs from binding to their target gene promoters to promote shade-induced gene expression (de Lucas et al. 2008, Feng et al. 2008).

The core jasmonic acid (JA)-signaling module consists of the JA receptor COI1, a subset of jasmonate–ZIM-domain (JAZ) repressor proteins, and transcription factors involved in regulating the expression of JA-responsive genes (Howe et al. 2018). In the presence of the bioactive form of JA, the protein interaction between COI1 and JAZ is facilitated, and the JAZ proteins are subsequently ubiquitinated by the SCF^{COI1} complex and degraded through the 26S proteasome pathway and then activate the expression of JA-responsive genes mediated in part by MYC2 transcription factor (Kazan and Manners 2011, Pauwels and Goossens 2011, Howe et al. 2018).

Intensive cross-talk between GA and JA signaling is involved to solve the allocation trade-off between growth and defense in shade (Ballaré and Pierik 2017). The molecular mechanism for this hormone cross-talk has been well studied and relies on the balance originating in the physical interaction between GA-dependent DELLA repressors and JA-dependent JAZ repressors. The activation of the JA pathway in response to plant defense results in JAZ degradation and an increase in DELLA activity, repressing growth (Yang et al. 2012, Hou et al. 2015). In contrast, the activation of the GA signaling in shade results in a reduction of DELLA levels and subsequent activation of the JAZ repressors, reducing the response to JA-mediated stimuli (Cerrudo et al. 2012, Chico et al. 2014, Leone et al. 2014).

B-box (BBX)-containing zinc finger transcription factors mediate transcriptional regulation and protein–protein interactions in plant development, often integrating environmental information with hormone signaling (Gangappa and Botto 2014, Song et al. 2020, Yadav et al. 2020). Interestingly, BBX24 modulates the activity of GA signaling by interacting physically with DELLA proteins, thereby enhancing PIF4 activity in the SAS (Crocco et al. 2015). More recently, it has been shown that BBX24 can also regulate the JA signaling pathway in sweet potatoes (Zhang et al. 2020). IbBBX24 represses the expression of IbJAZ10 by the protein–protein interaction and subsequently activates the expression of IbMYC2 by directly binding to their promoters to increase Fusarium wilt resistance (Zhang et al. 2020).

Despite the involvement of BBX24 in the SAS responses, only the interaction with GAs has been elucidated so far (Crocco et al. 2015). To generate a more comprehensive and complete view of the BBX24 mechanism related to SAS-induced responses, we studied the BBX24-dependent interactome and identified new relevant interactions. Here, we demonstrated the relevance of the BBX24 and JAZ3 protein interaction in the promotion of growth by reducing DELLA activity downstream of the phyB activity. These results suggest that BBX24 is an integrator of GA and JA signaling pathways for the promotion of hypocotyl growth in shade light.

Results

Interactome and transcriptome analyses suggest a link between BBX24 and JA signaling

To identify transcription factors that interact with BBX24, we performed a yeast-two-hybrid (Y2H) screening using the BBX24 protein as bait against a library of 1,956 *Arabidopsis thaliana* transcription factors (Pruneda-Paz Jose et al. 2014). We identified 60 likely positive interactions (**Supplementary Table S1**). The BBX24 interactors belong to 25 out of the 98 transcription factor families represented in the library (**Fig. 1**, **Supplementary Table S1**). Functionally, the 60 transcription factors are associated with multiple processes. Some of them are involved in abiotic or biotic stress responses (WRKY60, HSF3 and MYB2), light signaling (ZML2 and BBX23), flowering development (FBH4, APL and AGL16) and phytohormone signaling pathways including JA (JAZ3), auxin (IAA13, IAA4 and IAA27), brassinosteroid (BZS1 and BIM1) and cytokinin (CRF9), among others (**Fig. 1**). These results suggest that a common theme for many BBX24 interactors is their participation in hormone-regulated processes.

As an additional criterion to assess the biological relevance of these BBX24-dependent interactions, we reanalyzed the transcriptomic dataset of Col-0 and *bbx24-1* mutant seedlings grown in shade (Crocco et al. 2015). We found 370 genes differentially expressed between Col-0 and the *bbx24-1* mutant ($|\log_2 FC| \geq 0.6$, where FC is fold change). From those genes regulated by BBX24, we found 54 and 351 genes that are differentially expressed in the *bbx24-1* mutant compared to Col-0 at high and low R:FR ratios, respectively (**Supplementary**

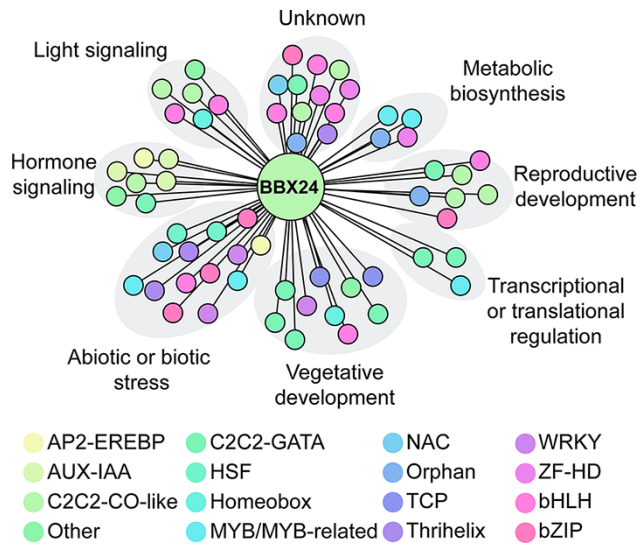

Fig. 1 Identification of transcription factors interacting with the BBX24 protein. Visualization of transcription factors interacting with partners of BBX24 identified in a Y2H screening. BBX24 protein interactors are represented as nodes and colored depending on their transcription factor family. Interactors are grouped according to their biological function.

Table S2). These results suggest that BBX24 plays a prominent role in shade light because it regulates a higher number of genes under this light condition than in white light (i.e. 6.5-folds) with a strong enrichment of genes falling in functional categories related to defense, biotic and stress responses (Fig. 2A, Supplementary Table S2). Given the known interaction between shade and JA signaling pathways, we compared the BBX24-dependent (Crocco et al. 2015) and methyl jasmonate (MeJA)-dependent transcriptomes (ArrayExpress-E-GEOD-21762) of *Arabidopsis* seedlings. We found a statistically significant convergence of genes co-regulated by MeJA- and BBX24-regulated genes in low but not in high R:FR ratios ($P = 3.15 \times 10^{-24}$ vs. 0.061, respectively; Fig. 2B, Supplementary Table S2). The gene ontology analysis showed that the commonly regulated genes are enriched in biological processes related to secondary metabolic processes, response to stress, defense response to insects and response to JA, among others (Supplementary Table S2). Among the 53 co-regulated genes, we found some members of the *XYLOGLUCAN ENDOTRANSGLUCOSYLASE/HYDROLASE* family (*XTH12* and *XTH26*) and arabinogalactan protein gene family (*AGP30* and *FLA6*), described previously as robust markers of hypocotyl growth in response to low R:FR ratios (Kohnen et al. 2016). Furthermore, there are several members of glutathione S-transferase (*GSTU4*, *GSTU11*, *GSTU24* and *GSTU25*). It has been documented that some members of the GSTU family are connected with phytochromes and JA signaling in the control of the hypocotyl growth in *Arabidopsis* (Jiang et al. 2010, Chen et al. 2017).

JAZ3 and BBX24 promote hypocotyl growth in shade

To better understand the finding convergence between JA- and BBX24-regulated genes in the Y2H screening and comparative transcriptome analysis, we evaluated the hypocotyl length in Col-0, *bbx24-1* and two independent BBX24 overexpressing lines in a medium with different MeJA concentrations at high and low R:FR ratios (Fig. 2C, Supplementary Fig. S1). After de-etiolation, the *Arabidopsis* seedlings were grown in white light or simulated shade for 4 d. In white light, the hypocotyl length was around 1.5 mm, independent of the genotype and the MeJA concentration used in the medium. However, we found significant effects of MeJA in a genotype-dependent manner in simulated shade (genotype × light × hormone, $P < 0.001$, Supplementary Fig. S1). The hypocotyl length was inhibited by MeJA in all genotypes, and the effects were higher for both BBX24-overexpressing lines and lower for *bbx24-1* seedlings. A concentration of as low as 1 μM MeJA was enough to abolish

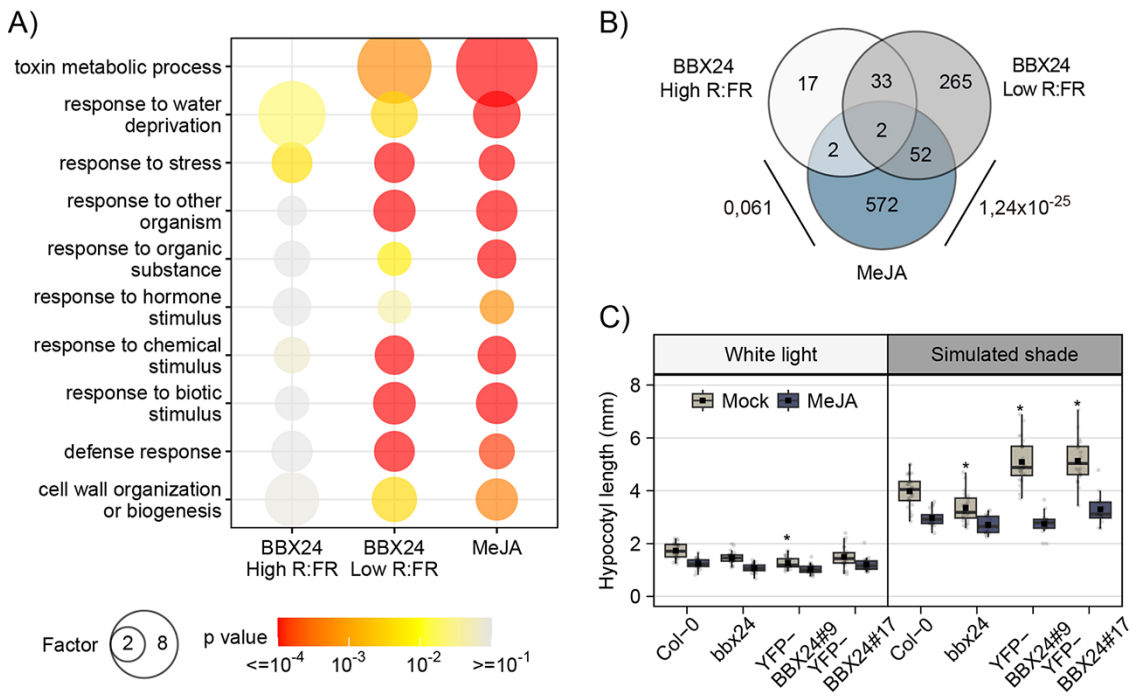

Fig. 2 Low R:FR ratios increase the overlap between the BBX24 function and JA signaling. (A) Gene ontology enrichment analysis of biological process terms comparing BBX24-regulated transcriptome, both at high R:FR and at low R:FR ratios, and MeJA-responsive transcriptome. Bubble size and color represent the enrichment factor and the adjusted *P*-value, respectively. (B) The Venn diagram shows overlapping between BBX24-regulated genes, both at high R:FR and at low R:FR ratios, and MeJA-regulated genes. The *P*-value of the overlap among groups of interest is shown. (C) Hypocotyl length of Col-0, *bbx24* and 35S:YFP-BBX24 #9 and #17 seedlings grown under white light or simulated shade treatment for 4 d under 1 μM MeJA or mock conditions. Boxplots show data obtained by the Tukey method ($n > 25$), and the mean is indicated as a square. Asterisks indicate that the difference is statistically significant with Col-0 under the same light and hormone conditions obtained by a two-way ANOVA followed by a post hoc test (Bonferroni correction, $P < 0.05$).

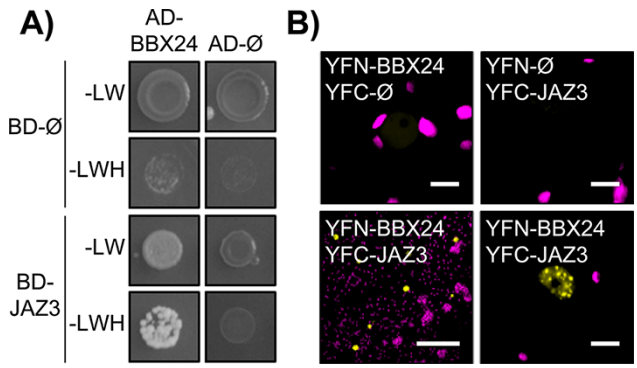

Fig. 3 Physical interactions between BBX24 and JAZ3 in vitro and in vivo. (A) The Y2H assay analyzing the interaction between JAZ3 and BBX24. (B) The BiFC assay in *N. benthamiana* leaves. Control leaves co-expressing YFN-BBX24/YFC and YFN/YFC-JAZ3 pairs (up) and leaves co-expressing BBX24 and JAZ3 fusions to N- and C-terminal fragments of YFP, respectively (bottom). The YFP signal is shown in yellow, and the chlorophyll autofluorescence is magenta. Scale bars, 100 μm (left panel YFN-BBX24 YFC-JAZ3) and 10 μm (rest of the panels).

the phenotype of BBX24 overexpression in the promotion of hypocotyl elongation under shade (**Fig. 2C**).

Previous evidence demonstrated the stabilization of other JAZ proteins (Chico et al. 2014) and the relevance of BBX24 interaction with DELLA proteins to promote PIF4 activity in shade (Crocco et al. 2015). Remarkably, we found in this work that (i) JAZ3 is a BBX24 interactor in the Y2H screening (**Fig. 1**, **Supplementary Table S1**), (ii) a high degree of convergence is observed between MeJA- and BBX24-dependent transcriptional targets particularly in shade instead of white light (**Fig. 2A, B**) and (iii) the interference is observed between MeJA- and BBX24-mediated hypocotyl growth in simulated shade but not in white light (**Fig. 2C**). Altogether, these findings suggest that the BBX24 and JAZ3 interaction could be implicated in phyB signaling in shade. To test this hypothesis and to have a better understanding of this possible functional connection, we confirmed the physical interaction between BBX24 and JAZ3 by two independent approaches, an independent Y2H assay (**Fig. 3A**) and a bimolecular fluorescence complementation (BiFC) assay in *Nicotiana benthamiana* leaves (**Fig. 3B**). As expected, the co-infiltration of JAZ3 and BBX24 proteins produced the yellow protein complementation but not in the negative controls. Furthermore, the interaction was observed in the nucleus of the cells, consistent with the expected localization of both JAZ3 and BBX24 proteins to be functional in shade (**Fig. 3B**).

In addition, we studied the *BBX24* and *JAZ3* expression in Col-0 seedlings supplemented with FR in white light. We found an increase of *BBX24* and *JAZ3* expression at 3-h FR, and then their expression descended significantly later at 5-h FR, suggesting an early induction of these genes in shade (**Supplementary Fig. S2**). The expression of *BBX24* was double induced than *JAZ3*, but both genes showed the same pattern of expression (**Supplementary Fig. S2**). These results suggest that the upregulation of *BBX24* and *JAZ3* expression could be necessary to promote the hypocotyl growth in shade light. To further confirm the physiological relevance of the BBX24 and JAZ3 physical interaction to promote hypocotyl growth in shade, we examined the phenotype of *bbx24-1 jaz3-4* double mutant seedlings. We designed two different experiments to evaluate hypocotyl growth in shade. In the first one, seedlings were grown below a green filter that reduced the PAR, blue and red photons (i.e. simulated shade). In the second one, a FR pulse was applied at the end of the photoperiod (end-of-day FR, EOD-FR), wich inactivates the phyB and other stable phytochromes and induce the shade-avoidance responses (Kasulin et al. 2013, Roig-Villanova and Martínez-García 2016). In both cases, we used white light as control treatment. The hypocotyl length of Col-0 seedlings significantly increased indistinctly in simulated shade and EOD-FR than in white light, while *bbx24-1* and *jaz3-4* single mutants showed shorter hypocotyls than Col-0 in shade but not in white light (**Fig. 4**). Mutating both genes simultaneously did not further affect the response to shade (**Fig. 4**), suggesting that both proteins regulate hypocotyl growth through a common signaling pathway mediated by phyB.

BBX24 and JAZ3 promote hypocotyl growth through GA signaling in shade

Low R:FR ratios and low blue photons typical of shaded environments enhance both GA biosynthesis and responsiveness in *Arabidopsis*, thereby promoting the expression of GA-related genes for the promotion of cell elongation (Hisamatsu et al. 2005, Djakovic-Petrovic et al. 2007). In a previous work, we found that BBX24 interacts with DELLA proteins, through the Leucine heptad repeat1 (LHR1) motif (Crocco et al. 2015). Here, we demonstrated that JAZ3 also interacts with DELLAs (**Supplementary Fig. S3**). The interaction requires the VHIID DELLA motif, but not the adjacent LHR1 motif (**Supplementary Fig. S3**). These results suggest that DELLAs sequester BBX24 and/or JAZ3, impeding the positive interaction between BBX24 and JAZ3 for the promotion of the hypocotyl growth in shade. To test this possibility, we examined the effect of altering GA levels by applying exogenous GA_3 or paclobutrazol (PAC), a GA biosynthesis inhibitor, on the hypocotyl length in *bbx24-1* and *jaz3-4* single mutants and *bbx24-1 jaz3-4* double mutants. In white light, all genotypes showed a similar hypocotyl length in mock, GA_3 and PAC treatments (**Fig. 5A**). In simulated shade, the untreated single mutants as well as *bbx24-1 jaz3-4* double mutants showed significantly shorter hypocotyls than Col-0, and the addition of GA_3 rescued the shorter hypocotyls of all mutants (**Fig. 5A**). The addition of PAC did not further reduce hypocotyl size in single and *bbx24-1 jaz3-4* double mutants (**Fig. 5A**). These results are compatible with our action model in which DELLA activity is high in the absence of BBX24 and JAZ3 and cannot be further stimulated by blocking GA-dependent DELLA degradation. To confirm our prediction, we generated the *bbx24-1 jaz3-4 gai-td1 rga-29* quadruple mutant. In white light, Col-0 and *bbx24-1 jaz3-4* seedlings showed slight but significantly shorter hypocotyls than the *gai-td1 rga-29* double

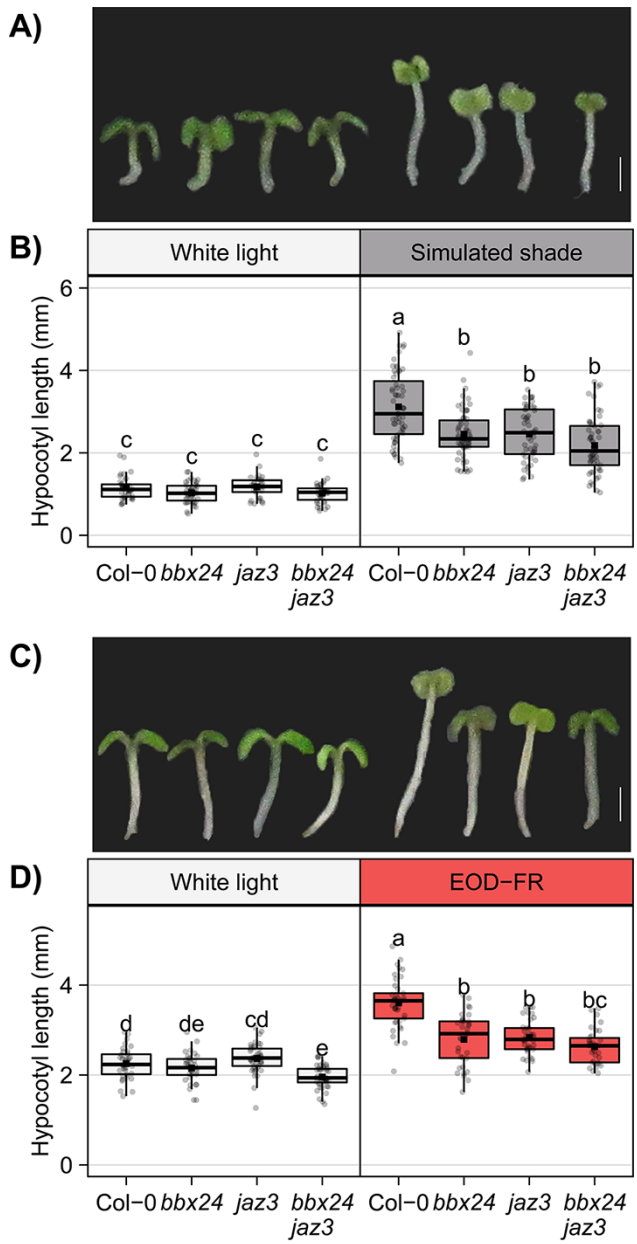

Fig. 4 BBX24 genetically interacts with JAZ3 to promote hypocotyl growth in shade. Phenotypic analysis of Col-0, *bbx24*, *jaz3* and *bbx24 jaz3* seedlings grown under (A, B) simulated shade or (C, D) EOD-FR treatment for 4 days. (A, C) Representative images of *Arabidopsis* seedlings. Scale bar, 1 mm. (B, D) Boxplots show data obtained by the Tukey method [(B) $n > 30$; (D) $n > 20$], and the mean is indicated as a square. Different letters indicate significantly different means obtained by a two-way ANOVA followed by the post hoc Tukey HSD ($P < 0.05$).

and *bbx24-1 jaz3-4 gai-td1 rga-29* quadruple mutants (**Fig. 5B**). In simulated shade, the shorter hypocotyls of *bbx24-1 jaz3-4* seedlings were completely rescued by loss of GIBBERELLIC-ACID INSENSITIVE (GAI) and REPRESSOR OF GAI (RGA) function (**Fig. 5B**).

We selected a set of genes co-regulated by BBX24 under shade and MeJA (**Supplementary Table S2**) to evaluate their expression in Col-0 and *bbx24-1*, *jaz3-4*, *bbx24-1 jaz3-4*, *gai-td1 rga-29* and *bbx24-1 jaz3-4 gai-td1 rga-29* seedlings growing under white light or simulated shade for 5 d (**Fig. 5C**). Two genes related to defense responses, *SDA1* and *GSTU4*, presented a major induction under shade in all the genotypes compared to Col-0 seedlings. On the other hand, *XTH26* was upregulated under shade in *bbx24-1*, *jaz3-4* and *bbx24-1 jaz3-4* mutants, but its expression was downregulated at the same levels of wild-type in *gai-td1 rga-29* double and *bbx24-1 jaz3-4 gai-td1 rga-29* quadruple mutants. *XTH12* and *XTH26* showed a similar pattern of gene expression, but we did not find statistically significant differences for *bbx24-1*, *jaz-3* single mutants and *bbx24-1 jaz-3* double mutants with Col-0 ($P \approx 0.10$). Altogether, these results suggest that the lack of GAI and RGA proteins rescues the impaired transcriptional regulation of genes related to hypocotyl growth in the *bbx24-1 jaz3-4* double mutant, but the possible implication of BBX24 and JAZ3 regulating defense under shade could involve a different mechanism independent of DELLA proteins.

BBX24 and JAZ3 converge with phyB to promote hypocotyl growth in shade

The phyB inactivation promotes hypocotyl growth by enhancing PIF4 activity and increasing GA biosynthesis, resulting in DELLA degradation (Djakovic-Petrovic et al. 2007, Pacín et al. 2016, Blanco-Touriñán et al. 2020). If JAZ3 and BBX24 jointly promote growth by inactivating DELLAs, the prediction of our model is that loss of phyB function should be epistatic to the loss of BBX24 and JAZ3 activities. Indeed, in white light, *phyB* and *bbx24-1 jaz3-4 phyb* seedlings showed longer hypocotyls than Col-0, and the shorter hypocotyl defect of *bbx24-1 jaz3-4* seedlings was partially rescued by the *phyB* mutation (**Fig. 6A**). Moreover, the inhibition of hypocotyl length by increasing doses of PAC was more pronounced in Col-0 and *bbx24-1 jaz3-4* than in *phyb* and *bbx24-1 jaz3-4 phyB* seedlings (**Fig. 6B**). The enhanced sensitivity of *phyB* seedlings to DELLA accumulation in the absence of JAZ3 and BBX24 agrees with the model of action in which JAZ3 and BBX24 activities converge for downregulation of DELLA to promote the hypocotyl growth in simulated shade downstream of phyB.

Discussion

Integration of external cues with developmental programs depends on phytohormone networks and is critical for plants to survive in nature. The reduction in R:FR ratios that occurs in dense canopies due to the absorption of R light by chlorophylls and reflection of FR light is an anticipatory signal of the presence of neighboring plant competitors (Ballaré et al. 1990, Ballaré and Pierik 2017). In fully de-etiolated plants, the low R:FR ratios, a direct estimator of plant density, inactivate phyB, which promotes growth to reach the light resource to maximize photosynthesis (Smith 1982, Casal 2013). The evidence presented in this work demonstrated that the plant growth promoted by simulated shade involves the participa-

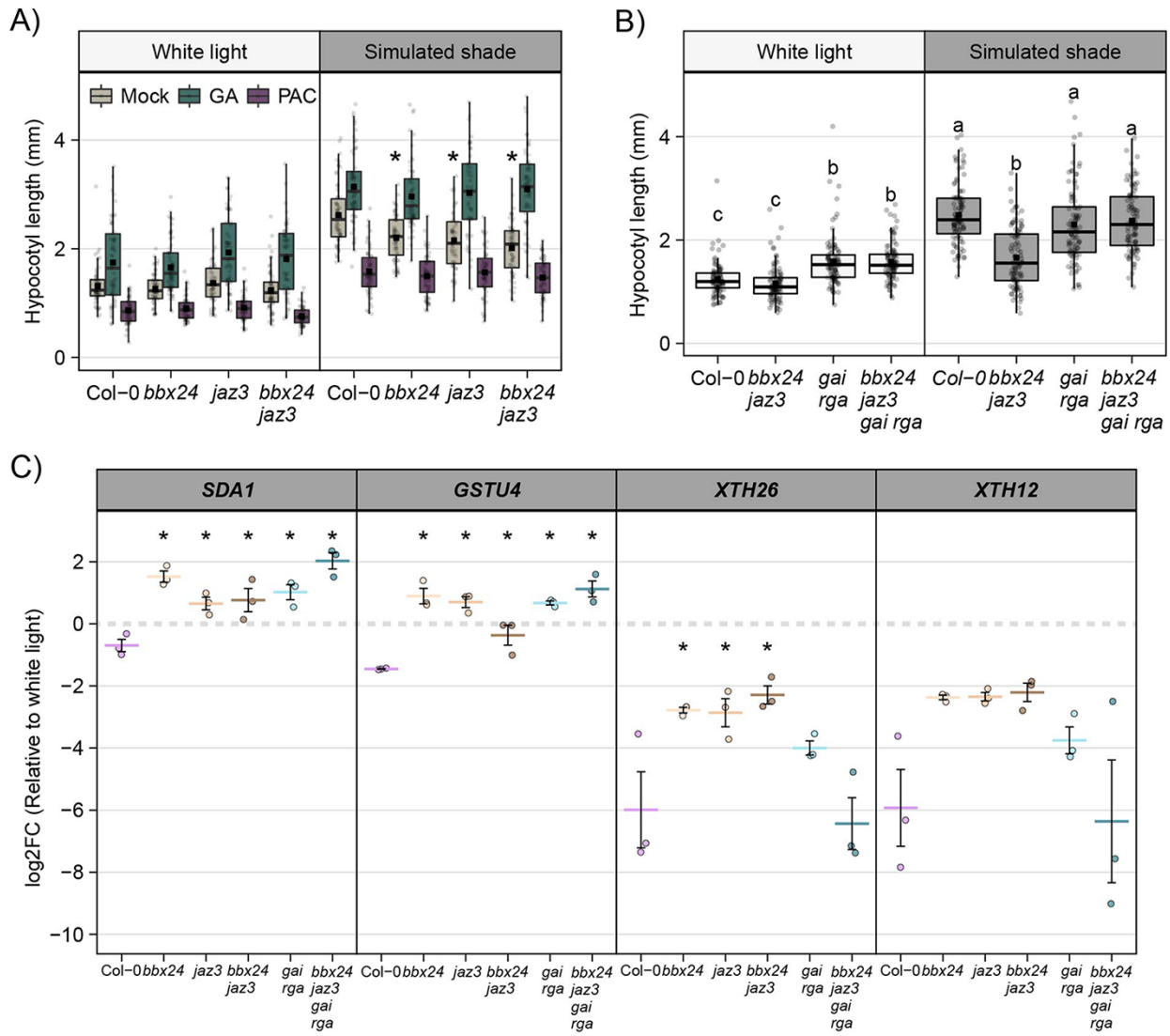

Fig. 5 BBX24 and JAZ3 promote hypocotyl growth through DELLA activity. (A) Hypocotyl length of Col-0, *bbx24*, *jaz3* and *bbx24 jaz3* seedlings grown under white light or simulated shade for 4 d incubated with 2 μM of GA, 1 μM PAC or mock. Boxplots show data obtained by the Tukey method ($n > 50$), and the mean is indicated as a square. Asterisks indicate that the difference is statistically significant with Col-0 under the same light and hormone condition obtained by a two-way ANOVA followed by a post hoc test (Bonferroni correction, $P < 0.05$). (B) Hypocotyl length of Col-0, *bbx24 jaz3*, *gai rga* and *gai rga bbx24 jaz3* seedlings grown under simulated shade treatment for 4 d. Boxplots show data obtained by the Tukey method ($n > 90$), and the mean is indicated as a square. Different letters indicate significantly different means obtained by a two-way ANOVA followed by the post hoc Tukey HSD ($P < 0.05$). (C) Transcript levels of *SDA1*, *GSTU4*, *XTH26* and *XTH12* genes were determined in Col-0, *bbx24*, *jaz3*, *bbx24 jaz3*, *gai rga* and *gai rga bbx24 jaz3* seedlings after 5 d under white light or simulated shade. Expression levels are relative to *UBQ10* and the log2FC induction under simulated shade relative to white light for genotype. Every dot represents a biological replicate, and the cross bars represent the mean and the standard deviation. Asterisks indicate significantly different means compared with Col-0 obtained by a one-way ANOVA followed by a post hoc test (Bonferroni correction, $P < 0.05$).

tion of JA signaling, as indicated by the reduced hypocotyl elongation of *jaz3* mutants (**Fig. 4**). Although the JA phytohormone had been previously proposed to be involved in the inhibition of the hypocotyl growth in simulated shade based on the exogenous application of MeJA (**Fig. 2**) (Chen et al. 2013), here we also demonstrated that JAZ3 is biologically relevant together with BBX24 in the phyB signaling pathway, both converging on the regulation of DELLA activity (**Figs. 4–6**). Furthermore, our model of the BBX24-JAZ3-DELLA module of action in simulated shade predicts that the loss of phyB function is epistatic to the loss of BBX24 and JAZ3 activities. Indeed, the shorter hypocotyl defect of *bbx24-1 jaz3-4* seedlings in shade was completely rescued by the *phyB* mutation (**Fig. 6A**). The enhanced sensitivity of *phyB* seedlings to DELLA accumulation in the absence of JAZ3 and BBX24 with the addition of PAC (**Fig. 6B**) agrees with the model in which JAZ3 and BBX24

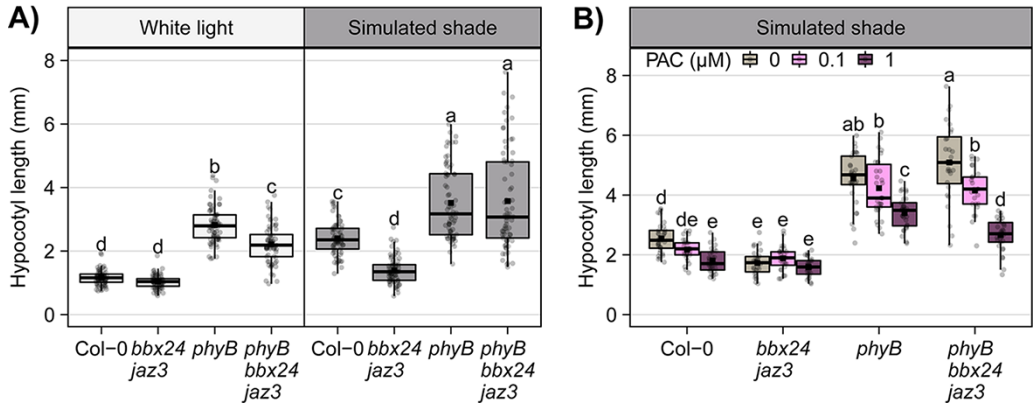

Fig. 6 phyB-BBX24-JAZ3 module regulates hypocotyl growth through GA signaling in shade. Hypocotyl length of Col-0, *bbx24 jaz3*, *phyB* and *phyB bbx24 jaz3* seedlings grown (A) under white light or simulated shade treatment for 4 d or (B) under simulated shade treatment for 4 d at different concentrations of PAC. Boxplots show data obtained by the Tukey method [(A) $n > 60$ and (B) $n > 30$], and the mean is indicated as a square. Different letters indicate significantly different means obtained by a two-way ANOVA followed by the post hoc Tukey HSD ($P < 0.05$).

activities converge for downregulation of DELLA activity to promote the hypocotyl growth in the phyB-mediated SAS signaling pathway.

The role of JAZ3 in the modulation of DELLA activity in response to simulated shade agrees with previous observations of other members of JAZ (Chico et al. 2014, Leone et al. 2014). Our results suggest that the physical interaction between JAZ3 and BBX24 (**Fig. 3**) contributes, at least in part, to connecting light information to JA signaling for the control of hypocotyl growth in shade (**Figs. 4–6**). We found that the lack of GAI RGA rescues the impaired expression regulation of genes related to cell elongation in the *bbx24-1 jaz3-4* double mutant, but the possible implication of BBX24 and JAZ3 regulating defense responses under shade appears to be independent of DELLA proteins (**Fig. 5**). It has been previously shown that FR-enriched white light triggers RGA protein degradation and increases JAZ10 protein stability, producing a rapid change in the balance between DELLA and JAZ proteins and allowing the reconfiguration of their resource allocation from defense to growth (Leone et al. 2014). Furthermore, our findings are in concordance with the JAZ protein stabilization in FR-enriched white light previously documented in *Arabidopsis* plants constitutively expressing JAZ proteins, including JAZ1, JAZ7, JAZ9, JAZ10, JAZ11 and JAZ12 (Chico et al. 2014). Further analysis could be performed to integrate the probable function of JAZ3 and BBX24 proteins in the JA regulation in plant immune response and shade light. Interestingly, a recent study in sweet potatoes reported the first evidence that connects BBX24 and JA defense responses. Indeed, overexpression of IbBBX24 promotes the activity of the JA signaling by the promotion of IbMYC2 transcription favored by the physical interaction between IbBBX24 and IbJAZ10 that enhances the resistance to *Fusarium* wilt (Zhang et al. 2020). Therefore, elucidation of the mechanism of JAZ3-BBX24-DELLA module activity in the trade-off between growth and plant defense may be complex and will require further research.

Simulated shade promotes phyB inactivation and DELLA degradation, resulting in the relief of PIF transcription factors to promote hypocotyl growth (Djakovic-Petrovic et al. 2007, Leone et al. 2014). Recent molecular evidence further indicates that BBX24 physically interacts with GAI and RGA DELLA proteins and facilitates the activation of transcriptional expression mediated by PIF4 to promote the elongation response in shade (Crocco et al. 2015). In addition, COP1 can directly regulate DELLA protein stability, because DELLA is targeted for degradation by COP1 in response to shade light (Blanco-Touriñán et al. 2020). Remarkably, BBX24 is genetically epistatic to COP1 in shade light and can be targeted for 26S proteasome–mediated degradation in a COP1-dependent manner (Gangappa et al. 2013). Furthermore, COP1/SPA activity also affects the abundance of negative modulators of shade-regulated growth including BBX proteins such as BBX21 and BBX22 (Crocco et al. 2010, Xu et al. 2016) and bHLH proteins such as HFR1 and PAR1 (Sessa et al. 2005, Hornitschek et al. 2009). Overall, these mechanisms not only tend to activate PIF transcription factors promoting elongation in shade but also lead to the activation of inhibitors implicated in negative feedback loops required for the precise adjustment of plant growth. Further studies are required to decipher the mechanism of BBX24 activity in COP1 signaling for the balance among antagonistic signals that become integrated by protein interactions in the SAS.

The screening of putative BBX24 interactors provided in this study suggests that BBX24 is involved in multiple physiological responses through different signaling networks (**Fig. 1**, **Supplementary Table S1**). The Y2H screening revealed that BBX24 can interact with transcription factors that are associated with response to biotic and abiotic stress, such as ERF53 in drought tolerance (Cheng et al. 2012), MYB76 in the production of aliphatic glucosinolates (Gigolashvili et al. 2008), HSF3 in anoxia (Banti et al. 2010), or HSF3A in thermotolerance (Schramm et al. 2008). In addition, BBX24 can interact with Aux/IAA

transcriptional regulators which operate as repressors in the auxin signaling pathway (Leyser 2018). BBX24 can also interact with proteins associated with light signaling responses including PIF3, BBX11 and BBX23. Altogether, our interactome analysis agrees with the multiple functions of BBX24 in the whole cycle of life of plants. BBX24 has been implicated in the inhibition of seedling de-etiolation (Indorf et al. 2007, Yan et al. 2011, Gangappa et al. 2013) and ultraviolet B responses (Jiang et al. 2012, Lyu et al. 2020). BBX24 has also been involved in the flowering of *Arabidopsis* (Li et al. 2014), tolerance to chilling and drought in overexpressing lines of chrysanthemum (Yang et al. 2014) and pigment coloration of pear fruits (Ou et al. 2020). Very recently, it has been demonstrated that JA and BBX are involved in the cold stress response in apples. In fact, MdJAZ1 and MdJAZ22 interact negatively with MdBBX37 to avoid JA-mediated cold tolerance (An et al. 2021). Overall, further studies will be focused to decipher the functional relevance of BBX24–protein interactions in response to light, hormone and biotic and abiotic stimuli, among others. In summary, we propose that BBX24 may act as a hub connecting different signaling pathways through rapid and reversible protein–protein interactions for the fine-tuning of plant growth and development in different environmental scenarios.

Materials and Methods

Plant materials

The experiments were performed with *A. thaliana* (L.) Heynh. Columbia (Col-0). The mutant lines *bbx24-1* (SALK_067473) (Indorf et al. 2007), *jaz3-4* (GK-097F09) (Campos et al. 2016), *gai-td1 rga-29* (*GAI*: SAIL_82_F06, *RGA*: SALK_089146) (Cagnola et al. 2018) and *phyB* (SALK_069700) (Alonso et al. 2003) (Seo et al. 2006) were previously described. The double and multiple mutant lines *bbx24-1 jaz3-4*, *bbx24-1 jaz3-4 gai-td1 rga-29* and *phyB bbx24-1 jaz3-4* were obtained by simple crossing and were identified by PCR using the primers listed in **Supplementary Table S3**.

To obtain the yellow fluorescent protein (YFP) transgenic line 35S:YFP-BBX24, *Agrobacterium tumefaciens* GV3101 cells were transformed with pEarleyGate104·BBX24 plasmid and introduced into *A. thaliana* Col-0 plants via the floral dip method (Zhang et al. 2006). Transgenic plants were selected on Murashige and Skoog's medium containing 15 mg/l Basta (T0 plants). The next generation (T1 plants) was selected under the same conditions and had only kept these lines with a 3:1 resistance ratio to ensure the presence of the transgene. Seeds of T3 generation of two independent homozygous lines (#9 and #17) were used for the experiments.

Growth conditions and physiological and pharmacological experiments

Seeds were sown in clear plastic boxes on 0.8% agar/water and incubated in darkness at 4°C. After 4 d, imbibed seeds were exposed to a white light pulse for 5 h and kept in darkness for 14 h at 22°C to induce germination. Then, the boxes were transferred to a short-day photoperiod (10 h/14 h) at 22°C and maintained for 2 d in white light to ensure complete de-etiolation. On the third day, the boxes were transferred to the corresponding light treatment for four additional days in the same photoperiod.

For hormone experiments, the same procedure was followed, but seeds were sown on a paper filter above the 0.8% agar/water medium. At the beginning of the night before the first day of treatment, the filter paper was transferred to an agar/water medium (0.8% v/v) supplemented with gibberellic acid (GA_3), PAC or MeJA at the corresponding concentrations and kept in this medium during all the light treatment.

For simulated shade experiments, white light treatment consisted of a mixture of fluorescent and incandescent lamps (PAR = 90 μmol m^{-2} s^{-1}, red = 9.1 μmol m^{-2} s^{-1}, blue = 8.1 μmol m^{-2} s^{-1} and FR = 8.3 μmol m^{-2} s^{-1}). Simulated shade (PAR = 20 μmol m^{-2} s^{-1}, red = 0.8 μmol m^{-2} s^{-1}, blue = 1.3 μmol m^{-2} s^{-1} and FR = 5.5 μmol m^{-2} s^{-1}) treatment was provided by the same light sources in combination with a green acetate filter (**Supplementary Fig. S4**, #089; LEE filters, http://www.leefilters.com) (Pacín et al. 2013). For EOD-FR experiments, the protocol was described previously with some modifications (Mizuno et al. 2015). *Arabidopsis* seedlings were grown in a Percival growth chamber with fluorescent lights (i.e. white light treatment, PAR = 90 μmol m^{-2} s^{-1}, red = 20 μmol m^{-2} s^{-1} and blue = 20 μmol m^{-2} s^{-1}). For EOD-FR treatment, an FR LED was placed on a lower shelf in the same growth chamber. The FR supplementation in the lower part reduced the ratio of R:FR to 0.25 without altering the intensity of PAR (PAR = 90 μmol m^{-2} s^{-1}, red = 10 μmol m^{-2} s^{-1}, blue = 10 μmol m^{-2} s^{-1} and FR = 40 μmol m^{-2} s^{-1}). From the first day of treatment, boxes were transferred manually from the upper part (white light treatment) to the lower part (EOD-FR treatment) of the chamber for the last 30 min of the photoperiod.

To measure the hypocotyl length, the boxes were placed vertically during the treatment and were photographed with a digital camera (PowerShot; Canon, http://www.canon.com). The hypocotyl length was determined using the Fiji distribution of ImageJ (Schneider et al. 2012).

Transcriptome analysis

To determine BBX24- and MeJA-regulated genes, E-GEOD-64755 (Crocco et al. 2015) and E-GEOD-21762 assays obtained from the ArrayExpress database (Athar et al. 2019) were used, respectively. For each assay, raw data (.CEL files) were downloaded and processed with Bioconductor and R. Quality data were analyzed using the *affyPLM* package and normalized by the Robust Multichip Average method using the *affy* package (Gautier et al. 2004, Bolstad 2015). Gene expression differential analysis was performed using a linear model with the *limma* package (Ritchie et al. 2015). To obtain BBX24-regulated genes, gene expression of *bbx24-1* mutant seedlings was compared with Col-0 seedlings grown under the same light condition (high or low R:FR). Genes with a >1.5-fold change in their expression (|log2FC|> 0.6) were selected. To obtain MeJA-regulated genes, gene expression of MeJA-treated seedlings was compared with mock-treated seedlings. Genes with a >2-fold change (|log2FC|> 1) and an adjusted *P*-value of <0.05 were selected.

Gene ontology enrichment analysis for biological process terms was performed using BioMaps from VirtualPlant 1.3 platform (Katari et al. 2010). The adjusted *P*-value was obtained using the Fisher exact test and corrected for multiple testing using the false discovery rate. The enrichment factor was estimated as the ratio of the proportion of genes associated with a particular term present in the dataset under analysis, relative to the number of genes in this category in all the probes of the ATH1 Affymetrix array. The bubble plot was generated using the *ggplot2* package in R (Wickham 2016). The Venn diagram was represented using the *VennDiagram* package in R (Chen and Boutros 2011). The statistical significance of the overlap between groups was obtained using an online tool (http://nemates.org/MA/progs/overlap_stats.html).

Y2H screening for the BBX24 interactome

Y2H screening was performed following a high throughput approach described earlier (Li et al. 2019). Briefly, AH109 (MATa), carrying the *PGA59-gLUC* reporter (Bonaldi et al. 2017) instead of *MEL1*, and YU (MATα) (Pruneda-Paz Jose et al. 2014) yeast strains were transformed with prey (pDEST22) and bait (pDEST32) vectors, respectively. Both yeast strains were mated in 384-well microplates (each well containing a single bait–prey pair). Luminescence and optical density at a wavelength of 600 nm (OD_{600}) for each well were determined in 384-well plates as described earlier (Li et al. 2019).

Two independent experiments were performed, each consisting of individually testing the interaction between 1,956 *Arabidopsis* transcription factors (cloned in pDEST22) (Pruneda-Paz Jose et al. 2014) and empty vector control (pEXP-AD502) (Life Technologies, California, United States) versus either BBX24 (cloned in pDEST32) or empty vector control (pDEST32-MCS). In each experiment, the PGA59-gLUC reporter activity was calculated for each well as the [(luminescence – mean blank)/(OD_{600} – mean OD_{600} blank)] ratio (blanks were obtained from cell-free wells in each microplate). Given that low OD_{600} values could artificially increase the reporter activity, raising false-positive calls, wells that exhibited a low OD_{600} (not statistically different from the average OD_{600} blank), were excluded from further analysis. To identify self-activating preys, a reporter activity self-activation cut-off value was calculated as (2× average + 3SD) of the PGA59-gLUC reporter activity obtained when pEXP-AD502 and pDEST32-MCS were prey and bait, respectively. Self-activating transcription factor preys (pDEST22-transcription factor versus pDEST32-MCS pairs that resulted in reporter activities above the self-activation reporter activity cut-off) were excluded from further analysis. To identify BBX24 interaction proteins, a reporter activity interaction cut-off value was calculated as (2× average + 4SD) of the PGA59-gLUC reporter activity obtained when pEXP-AD502 and pDEST32-BBX24 were prey and bait, respectively. Positive interactions were considered when a transcription factor–BBX24 pair exhibited a reporter activity above the interaction cut-off value. Interactome was visualized by Cytoscape (Smoot et al. 2011).

Y2H assay and plasmid constructions

The yeast strains, Y2H gold and Y187, were transformed with pDEST22 and pDEST32 constructions, respectively, by the LiAc/SS-DNA/PEG method (Gietz 2014). Transformed cells were grown in a YPD medium to facilitate mating. The diploid cells were selected and were used in –W–L or –W–L–H medium to identify positive interactions.

To obtain pZeo·BBX24 and pZeo·JAZ3 entry plasmids, *BBX24* coding DNA sequence (CDS) and *JAZ3* CDS (variant *JAZ3.1*) were amplified by PCR from cDNA of *A. thaliana* Col-0 using primers listed in **Supplementary Table S3**. The CDS sequences were cloned into pDONR Zeo plasmid (Invitrogen, Massachusetts, United States) by in vitro recombination of the PCR product and the donor vector. To obtain the YFP-BBX24 fusion protein, BBX24 CDS was transferred to the pEarleyGate104 LR reaction (Earley et al. 2006). To obtain yeast expression constructions, pDEST22 and pDEST32 plasmids (Invitrogen) were used. The BBX24 CDS and JAZ3 CDS were cloned into pDEST22 or pDEST32 plasmids to obtain the respective fusion proteins to the Gal4 activation domain (BBX24-AD and JAZ3-AD) and Gal4 DNA-binding domain (BBX24-BD and JAZ3-BD), using LR clonase (Life Technologies). The multiple cloning site of pUC19 was cloned into pDEST32 to obtain the pDEST32-MCS control vector. Expression plasmids containing GAI deletions were previously described in Gallego-Bartolomé et al. (2012). To obtain YFN·BBX24 and YFC·JAZ3, BBX24 CDS and JAZ3 CDS were transferred from entry plasmids to YFN43 and YFC43 by respective LR reactions (Belda-Palazón et al. 2012).

Bimolecular fluorescence complementation

The protocol was described previously (Belda-Palazón et al. 2012). *Agrobacterium tumefaciens* GV3101 cells were transformed with YFN·BBX24, YFC·JAZ3 or the empty vectors and were grown until $OD_{600} = 0.6$. Cells were precipitated and incubated into the infiltration solution ($MgCl_2$ 10 mM, MES 10 mM pH 5.6, acetosyringone 200 μM) for 3 h at 28°C. Cells were mixed to obtain the different pair combinations in a 1:1 ratio ($OD_{600} = 0.1$) and were used to infiltrate 4-week-old *N. benthamiana* leaves grown in a long-day photoperiod (16 h/8 h). After 2 d, the protein interaction was evaluated by confocal microscopy.

RT-qPCR analysis

For RNA expression, 100 mg of fresh seedlings was harvested and frozen immediately in liquid nitrogen. Total RNA was extracted using a Spectrum™ plant total RNA kit (Sigma-Aldrich, St. Louis, MO, USA). Crude RNA preparations were treated with 1.5 units of RNase-free DNase I (http://www.promega.com). cDNA was synthesized from 2 μg of DNA-free RNA template using an oligo(dT) primer and Moloney Murine Leukemia Virus reverse transcriptase (http://www.promega.com). RT-qPCR analysis was performed on an optical 96-well plate using LightCycler 480 SYBR Green I Master mix (Roche, https://www.roche.com/) and a LightCycler 480 II real-time PCR system (https://www.roche.com/). The thermal cycle used was 95°C for 5 min, followed by 40 cycles of 95°C for 15 s and 60°C for 1 min. Specific primer pairs for each gene were designed using NCBI Primer-BLAST (https://www.ncbi.nlm.nih.gov/tools/primer-blast/) and are listed in **Supplementary Table S3**.

Data analysis

In this paper, the statistical analysis was performed in R (R Core Team, 2022). For the ANOVA tests followed by the post hoc Tukey honestly significant difference (HSD), a linear model with the corresponding factors and the interaction among factors was performed using the function lm(), and the ANOVA was performed using the function aov(). Then, the post hoc Tukey HSD tests were performed using the emmeans (Lenth, et al., 2018) and multcomp (Hothorn et al. 2008) packages. For the ANOVA test followed by a comparison of means against the Col-0 genotype, the emmeans_test function was used and the adjust_pvalue function with the 'Bonferroni' method was used to correct the *P*-values.

Supplementary Data

Supplementary data are available at *PCP* online.

Data Availability

The data underlying this article will be shared on reasonable request to the corresponding author.

Funding

The University of Buenos Aires (UBACYT 2018–2021 20020170100265BA) and the Agencia Nacional de Promoción Científica y Tecnológica (PICT2017-0583 and PICT2019-2807) to J.F.B.; National Science Foundation (NSF) divisions Integrative Organismal Systems (IOS) and Molecular and Cellular Biosciences (MCB) (NSF IOS 1755452 and NSF MCB 1158254) and National Institute of Health (R01GM056006) to J.L.P.-P. and the European Union SIGNAT-Research and Innovation Staff Exchange (H2020-MSCA-RISE-2014-644435) to M.A.B. and J.F.B.

Acknowledgements

We thank Javier E. Moreno for the kind provision of the *jaz3-4* mutant line and Marcos Castellanos from the Nottingham Arabidopsis Stock Centre for the provision of seeds. We also thank Roberto Tornese for his technical assistance in the adjustment of light chambers for the experiments.

Author Contributions

M.S.-S. and J.F.B. conceived and designed the experiments; M.S.-S. performed the experiments with the help of T.S.C., J.C. and G.G.O. in genetic crosses and molecular and physiological experiments; J.H.-G. performed protein–protein interaction

PCP PLANT & CELL PHYSIOLOGY

assays; Z.L. and J.L.P.-P. generated the BBX24 interactome. J.L.P.-P. and M.A.B. contributed with reagents and materials. J.F.B. supervised the experiments and wrote the article with the contribution of M.S.-S. and M.A.B. All the authors read the manuscript.

Disclosures

The authors have no conflicts of interest to declare.

References

Alonso, J., Stepanova, A., Leisse, T., Kim, C., Chen, H., Shinn, P., et al. (2003) Genome-wide insertional mutagenesis of *Arabidopsis thaliana*. *Science* 301: 653–657.

An, J.P., Wang, X.F., Zhang, X.W., You, C.X. and Hao, Y.J. (2021) Apple B-box protein BBX37 regulates jasmonic acid mediated cold tolerance through the JAZ-BBX37-ICE1-CBF pathway and undergoes MIEL1-mediated ubiquitination and degradation. *New Phytol.* 229: 2707–2729.

Athar, A., Füllgrabe, A., George, N., Iqbal, H., Huerta, L., Ali, A., et al. (2019) ArrayExpress update—from bulk to single-cell expression data. *Nucleic Acids Res.* 47: D711–D715.

Ballaré, C.L. and Pierik, R. (2017) The shade-avoidance syndrome: multiple signals and ecological consequences. *Plant Cell Environ.* 40: 2530–2543.

Ballaré, C.L., Scopel, A.L. and Sánchez, R.A. (1990) Far-red radiation reflected from adjacent leaves: an early signal of competition in plant canopies. *Science* 247: 329–332.

Banti, V., Mafessoni, F., Loreti, E., Alpi, A. and Perata, P. (2010) The heat-inducible transcription factor HsfA2 enhances anoxia tolerance in *Arabidopsis*. *Plant Physiol.* 152: 1471–1483.

Belda-Palazón, B., Ruiz, L., Martí, E., Tárraga, S., Tiburcio, A.F., Culiáñez, F., et al. (2012) Aminopropyltransferases involved in polyamine biosynthesis localize preferentially in the nucleus of plant cells. *PLoS One* 7: e46907.

Blanco-Touriñán, N., Legris, M., Minguet, E.G. Costigliolo-Rojas, C., Nohales, M.A., Iniesto, E., et al. (2020) COP1 destabilizes DELLA proteins in *Arabidopsis*. *Proc. Natl. Acad. Sci.* 117: 13792–13799.

Bolstad, B. (2015) affyPLM: Model Based QC Assessment of Affymetrix GeneChips. https://bioconductor.riken.jp/packages/3.2/bioc/vignettes/affyPLM/inst/doc/QualityAssess.pdf (December 16, 2019, date last accessed).

Bonaldi, K., Li, Z., Kang, S.E., Breton, G. and Pruneda-Paz, J.L. (2017) Novel cell surface luciferase reporter for high-throughput yeast one-hybrid screens. *Nucleic Acids Res.* 45: e157.

Cagnola, J.I., Cerdán, P.D., Pacín, M., Andrade, A., Rodriguez, V., Zurbriggen, M.D., et al. (2018) Long-day photoperiod enhances jasmonic acid-related plant defense. *Plant Physiol.* 178: 163–173.

Campos, M.L., Yoshida, Y., Major, I.T., de Oliveira Ferreira, D., Weraduwage, S.M., Froehlich, J.E., et al. (2016) Rewiring of jasmonate and phytochrome B signalling uncouples plant growth-defense tradeoffs. *Nat. Commun.* 7: 12570.

Casal, J.J. (2013) Photoreceptor signaling networks in plant responses to shade. *Annu. Rev. Plant Biol.* 64: 403–427.

Cerrudo, I., Keller, M.M., Cargnel, M.D., Demkura, P.V., de Wit, M., Patitucci, M.S., et al. (2012) Low red/far-red ratios reduce *Arabidopsis* resistance to *Botrytis cinerea* and jasmonate responses via a COI1-JAZ10-dependent, salicylic acid-independent mechanism. *Plant Physiol.* 158: 2042–2052.

Chen, H. and Boutros, P.C. (2011) VennDiagram: a package for the generation of highly-customizable Venn and Euler diagrams in R. *BMC Bioinform.* 12: 35.

Cheng, M.C., Hsieh, E.J., Chen, J.H., Chen, H.Y. and Lin, T.P. (2012) *Arabidopsis* RGLG2, functioning as a RING E3 ligase, interacts with AtERF53 and negatively regulates the plant drought stress response. *Plant Physiol.* 158: 363–375.

Chen, C.Y., Ho, S.S., Kuo, T.Y., Hsieh, H.L. and Cheng, Y.S. (2017) Structural basis of jasmonate-amido synthetase FIN219 in complex with glutathione S-transferase FIP1 during the JA signal regulation. *Proc. Natl. Acad. Sci. USA* 114: E1815–E1824.

Chen, J., Sonobe, K., Ogawa, N., Masuda, S., Nagatani, A., Kobayashi, Y., et al. (2013) Inhibition of *Arabidopsis* hypocotyl elongation by jasmonates is enhanced under red light in phytochrome B dependent manner. *J. Plant Res.* 126: 161–168.

Chico, J.M., Fernández-Barbero, G., Chini, A., Fernández-Calvo, P., Díez-Díaz, M. and Solano, R. (2014) Repression of jasmonate-dependent defenses by shade involves differential regulation of protein stability of MYC transcription factors and their JAZ repressors in *Arabidopsis*. *Plant Cell* 26: 1967–1980.

Crocco, C.D., Holm, M., Yanovsky, M.J. and Botto, J.F. (2010) AtBBX21 and COP1 genetically interact in the regulation of shade avoidance. *Plant J.* 64: 551–562.

Crocco, C., Locascio, A.E., Alabadí, D., Blázquez, M. and Botto, J. (2015) The transcriptional regulator BBX24 impairs DELLA activity to promote shade avoidance in *Arabidopsis thaliana*. *Nat. Commun.* 6: 6202.

de Lucas, M., Daviére, J.M., Rodríguez-Falcón, M., Pontin, M., Iglesias-Pedraz, J.M., Lorrain, S., et al. (2008) A molecular framework for light and gibberellin control of cell elongation. *Nat. Lett.* 451: 480–486.

Djakovic-Petrovic, T., de Wit, M., Voesenek, L.A.C.J. and Pierik, R. (2007) DELLA protein function in growth responses to canopy signals. *Plant J.* 51: 117–126.

Earley, K.W., Haag, J.R., Pontes, O., Opper, K., Juehne, T., Song, K., et al. (2006) Gateway-compatible vectors for plant functional genomics and proteomics. *Plant J.* 45: 616–629.

Feng, S., Martinez, C., Gusmaroli, G., Wang, Y., Zhou, J., Wang, F., et al. (2008) Coordinated regulation of *Arabidopsis thaliana* development by light and gibberellins. *Nature* 451: 475–480.

Gallego-Bartolomé, J., Minguet, E.G. Grau-Enguix, F., Abbas, M., Locascio, A., Thomas, S.G., et al. (2012) Molecular mechanism for the interaction between gibberellin and brassinosteroid signaling pathways in *Arabidopsis*. *Proc. Natl. Acad. Sci.* 109: 13446–13451.

Gangappa, S.N. and Botto, J.F. (2014) The BBX family of plant transcription factors. *Trends Plant Sci.* 19: 460–470.

Gangappa, S.N., Crocco, C.D., Johansson, H., Datta, S., Hettiarachchi, C., Holm, M., et al. (2013) The *Arabidopsis* B-BOX protein BBX25 interacts with HY5, negatively regulating BBX22 expression to suppress seedling photomorphogenesis. *Plant Cell Online* 25: 1243–1257.

Gautier, L., Cope, L., Bolstad, B.M. and Irizarry, R.A. (2004) affy—analysis of Affymetrix GeneChip data at the probe level. *Bioinformatics* 20: 307–315.

Gietz, R.D. (2014) Yeast transformation by the LiAc/SS carrier DNA/PEG method. *Methods Mol. Biol. (Clifton, NJ)* 1163: 33–44.

Gigolashvili, T., Engqvist, M., Yatusevich, R., Müller, C. and Flügge, U.I. (2008) HAG2/MYB76 and HAG3/MYB29 exert a specific and coordinated control on the regulation of aliphatic glucosinolate biosynthesis in *Arabidopsis thaliana*. *New Phytol.* 177: 627–642.

Hisamatsu, T., King, R.W., Helliwell, C.A. and Koshioka, M. (2005) The involvement of gibberellin 20-oxidase genes in phytochrome-regulated petiole elongation of *Arabidopsis*. *Plant Physiol.* 138: 1106–1116.

Hornitschek, P., Lorrain, S., Zoete, V., Michielin, O. and Fankhauser, C. (2009) Inhibition of the shade avoidance response by formation of non-DNA binding bHLH heterodimers. *EMBO J.* 28: 3893–3902.

Hothorn, T., Bretz, F. and Westfall, P. (2008) Simultaneous inference in general parametric models. *Biom. J.* 50: 346–363.

Hou, X., Lee, L.Y.C., Xia, K., Yan, Y. and Yu, H. (2015) DELLAs modulate jasmonate signaling via competitive binding to JAZs. *Dev. Cell* 19: 884–894.

Howe, G.A., Major, I.T. and Koo, A.J. (2018) Modularity in jasmonate signaling for multistress resilience. *Annu. Rev. Plant Biol.* 69: 387–415.

Indorf, M., Cordero, J., Neuhaus, G. and Rodríguez-Franco, M. (2007) Salt tolerance (STO), a stress-related protein, has a major role in light signalling. *Plant J.* 51: 563–574.

Jiang, H.W., Liu, M.J., Chen, I.C., Huang, C.H., Chao, L.Y. and Hsieh, H.L. (2010) A glutathione S-transferase regulated by light and hormones participates in the modulation of *Arabidopsis* seedling development. *Plant Physiol.* 154: 1646–1658.

Jiang, L., Wang, Y., Li, Q.-F., Björn, L.O., He, J.-X. and Li, -S.-S. (2012) *Arabidopsis* STO/BBX24 negatively regulates UV-B signaling by interacting with COP1 and repressing HY5 transcriptional activity. *Cell Res.* 22: 1046–1057.

Kasulin, L., Agrofoglio, Y. and Botto, J.F. (2013) The receptor-like kinase ERECTA contributes to the shade-avoidance syndrome in a background-dependent manner. *Ann. Bot.* 111: 811–819.

Katari, M.S., Nowicki, S.D., Aceituno, F.F., Nero, D., Kelfer, J., Thompson, L.P., et al. (2010) VirtualPlant: a software platform to support systems biology research. *Plant Physiol.* 152: 500–515.

Kazan, K. and Manners, J.M. (2011) The interplay between light and jasmonate signalling during defence and development. *J. Exp. Bot.* 62: 4087–4100.

Kohnen, M.V., Schmid-Siegert, E., Trevisan, M., Petrolati, L.A., Sénéchal, F., Müller-Moulé, P., et al. (2016) Neighbor detection induces organ-specific transcriptomes, revealing patterns underlying hypocotyl-specific growth. *Plant Cell* 28: 2889–2904.

Lenth, R., Singmann, H., Love, J., Buerkner, P. and Herve, M. (2018) Package 'emmeans'. https://cran.microsoft.com/snapshot/2018-01-13/web/packages/emmeans/emmeans.pdf (December 23, 2019, date last accessed).

Leone, M., Keller, M.M., Cerrudo, I. and Ballaré, C.L. (2014) To grow or defend? Low red: far-red ratios reduce jasmonate sensitivity in *Arabidopsis* seedlings by promoting DELLA degradation and increasing JAZ10 stability. *New Phytol.* 204: 355–367.

Leyser, O. (2018) Auxin signaling. *Plant Physiol.* 176: 465–479.

Li, Z., Bonaldi, K., Kang, S.E. and Pruneda-Paz, J.L. (2019) High-throughput yeast one-hybrid screens using a cell surface gLUC reporter. *Curr. Protoc. Plant Biol.* 4: e20086.

Li, F., Sun, J., Wang, D., Bai, S., Clarke, A.K. and Holm, M. (2014) The B-box family gene STO (BBX24) in *Arabidopsis thaliana* regulates flowering time in different pathways. *PLoS One* 9: e87544.

Lyu, G., Li, D., Xiong, H., Xiao, L., Tong, J., Ning, C., et al. (2020) Quantitative proteomic analyses identify STO/BBX24-related proteins induced by UV-B. *Int. J. Mol. Sci.* 21: 2496.

McGinnis, K., Thomas, S., Soule, J., Strader, L., Zale, J., Sun, T.-P., et al. (2003) The *Arabidopsis* SLEEPY gene encodes a putative F-box subunit of an SCF E3 ubiquitin ligase. *Plant Cell* 15: 1120–1130.

Mizuno, T., Oka, H., Yoshimura, F., Ishida, K. and Yamashino, T. (2015) Insight into the mechanism of end-of-day far-red light (EODFR)-induced shade avoidance responses in *Arabidopsis thaliana*. *Biosci. Biotechnol. Biochem.* 79: 1987–1994.

Nakajima, M., Shimada, A., Takashi, Y., Kim, Y.-C., Park, S.-H., Ueguchi-Tanaka, M., et al. (2006) Identification and characterization of *Arabidopsis* gibberellin receptors. *Plant J.* 46: 880–889.

Ou, C., Zhang, X., Wang, F., Zhang, L., Zhang, Y., Fang, M., et al. (2020) A 14 nucleotide deletion mutation in the coding region of the *PpBBX24* gene is associated with the red skin of "Zaosu Red" pear (*Pyrus pyrifolia* White Pear Group): a deletion in the *PpBBX24* gene is associated with the red skin of pear. *Hortic. Res* 7: 39.

Pacín, M., Legris, M. and Casal, J.J. (2013) COP1 re-accumulates in the nucleus under shade. *Plant J.* 75: 631–641.

Pacín, M., Semmoloni, M., Legris, M., Finlayson, S.A. and Casal, J.J. (2016) Convergence of CONSTITUTIVE PHOTOMORPHOGENESIS 1 and PHYTOCHROME INTERACTING FACTOR signalling during shade avoidance. *New Phytol.* 211: 967–79.

Pauwels, L. and Goossens, A. (2011) The JAZ proteins: a crucial interface in the jasmonate signaling cascade. *Plant Cell* 23: 3089–3100.

Phokas, A. and Coates, J.C. (2021) Evolution of DELLA function and signaling in land plants. *Evol. Dev.* 23: 137–154.

Pruneda-Paz Jose, L., Breton, G., Nagel Dawn, H., Kang, S.E., Bonaldi, K., Doherty Colleen, J., et al. (2014) A genome-scale resource for the functional characterization of *Arabidopsis* transcription factors. *Cell Rep.* 8: 622–632.

R Core Team. (2022) R: A language and environment for statistical computing. R Foundation for Statistical Computing, Vienna, Austria. https://www.R-project.org/ (May 23, 2022, date last accessed).

Ritchie, M.E., Phipson, B., Wu, D., Hu, Y., Law, C.W., Shi, W., et al. (2015) limma powers differential expression analyses for RNA-sequencing and microarray studies. *Nucleic Acids Res.* 43: e47.

Roig-Villanova, I. and Martínez-García, J.F. (2016) Plant responses to vegetation proximity: a whole life avoiding shade. *Front. Plant Sci.* 7: 236.

Schneider, C.A., Rasband, W.S. and Eliceiri, K.W. (2012) NIH Image to ImageJ: 25 years of image analysis. *Nat. Methods* 9: 671–675.

Schramm, F., Larkindale, J., Kiehlmann, E., Ganguli, A., Englich, G., Vierling, E., et al. (2008) A cascade of transcription factor DREB2A and heat stress transcription factor HsfA3 regulates the heat stress response of *Arabidopsis*. *Plant J.* 53: 264–274.

Seo, M., Hanada, A., Kuwahara, A., Endo, A., Okamoto, M., Yamauchi, Y., et al. (2006) Regulation of hormone metabolism in *Arabidopsis* seeds: phytochrome regulation of abscisic acid metabolism and abscisic acid regulation of gibberellin metabolism. *Plant J.* 48: 354–366.

Sessa, G., Carabelli, M., Sassi, M., Ciolfi, A., Possenti, M., Mittempergher, F., et al. (2005) A dynamic balance between gene activation and repression regulates the shade avoidance response in *Arabidopsis*. *Genes Dev.* 19: 2811–2815.

Smith, H. (1982) Light quality, photoperception and plant strategy. *Annu. Rev. Plant Physiol.* 33: 481–518.

Smoot, M.E., Ono, K., Ruscheinski, J., Wang, P.L. and Ideker, T. (2011) Cytoscape 2.8: new features for data integration and network visualization. *Bioinformatics* 27: 431–432.

Song, Z., Bian, Y., Liu, J., Sun, Y. and Xu, D. (2020) B-box proteins: pivotal players in light-mediated development in plants. *J. Integr. Plant Biol.* 62: 1293–1309.

Ueguchi-Tanaka, M., Ashikari, M., Nakajima, M., Itoh, H., Katoh, E., Kobayashi, M., et al. (2005) GIBBERELLIN INSENSITIVE DWARF1 encodes a soluble receptor for gibberellin. *Nature* 437: 693–698.

Wickham, H. (2016) ggplot2: Elegant Graphics for Data Analysis. https://ggplot2.tidyverse.org (December 26, 2019, date last accessed).

Xu, D., Jiang Y, Lib, J., Lina, F., Holm, M. and Deng, X.W. (2016) BBX21, an *Arabidopsis* B-box protein, directly activates HY5 and is targeted by COP1 for 26S proteasome-mediated degradation. *Proc. Natl. Acad. Sci.* 113: 7655–60.

Yadav, A., Ravindran, N., Singh, D., Rahul, P.V. and Datta, S. (2020) Role of *Arabidopsis* BBX proteins in light signaling. *J. Plant Biochem. Biotechnol.* 29: 623–635.

Yang, C. and Li, L. (2017) Hormonal regulation in shade avoidance. *Front. Plant Sci.* 8: 1527.

Yang, Y., Ma, C., Xu, Y., Wei, Q., Imtiaz, M., Lan, H., et al. (2014) A zinc finger protein regulates flowering time and abiotic stress tolerance in

chrysanthemum by modulating gibberellin biosynthesis. *Plant Cell* 26: 2038.

Yang, D.-L., Yao, J., Mei, C.-S., Tong, X.-H., Zeng, L.-J., Li, Q., et al. (2012) Plant hormone jasmonate prioritizes defense over growth by interfering with gibberellin signaling cascade. *Proc. Natl. Acad. Sci.* 109: E1192–E1200.

Yan, H., Marquardt, K., Indorf, M., Jutt, D., Kircher, S., Neuhaus, G., et al. (2011) Nuclear localization and interaction with COP1 are required for STO/BBX24 function during photomorphogenesis. *Plant Physiol.* 156: 1772–1782.

Zhang, X., Henriques, R., Lin, S.-S., Niu, Q.-W. and Chua, N.-H. (2006) *Agrobacterium*-mediated transformation of *Arabidopsis thaliana* using the floral dip method. *Nat. Protoc.* 1: 641–646.

Zhang, H., Zhang, Q., Zhai, H., Gao, S., Yang, L., Wang, Z., et al. (2020) IbBBX24 promotes the jasmonic acid pathway and enhances Fusarium wilt resistance in sweet potato. *Plant Cell* 32: 1102–1123.